



Nematicity, magnetic fluctuation and ferro-spin-orbital ordering in BaFe_2As_2 family



Smritijit Sen ^{a, b}, Haranath Ghosh ^{a, b, *}

^a Homi Bhabha National Institute, Anushaktinagar, Mumbai 400 094, India

^b Indus Synchrotrons Utilization Division, Raja Ramanna Centre for Advanced Technology, Indore 452013, India

ARTICLE INFO

Article history:

Received 30 November 2015

Received in revised form

21 February 2016

Accepted 6 March 2016

Available online 9 March 2016

Keywords:

Fe-based superconductors

Orbital fluctuation

Nematicity

Spin density wave

ABSTRACT

Through detailed electronic structure simulations we show that the electronic orbital ordering (between d_{yz} and d_{xz} bands) takes place due to local breaking of in-plane symmetry that generates two non-equivalent a , b directions in 122 family of Fe-based superconductors. Orbital ordering is strongly anisotropic and the temperature dependence of the corner zone orbital order maps to that of the orthorhombicity parameter. Orbital anisotropy results in two distinct spin density wave nesting wave vectors and causes inter-orbital charge and spin fluctuations. Temperature dependence of the orbital order is proportional to the nematic order and it sets in at a temperature where magnetic fluctuation starts building. Magnetic fluctuations in the orthorhombic phase is characterized through evolution of Stoner factor which reproduces experimental findings very accurately. Orbital ordering becomes strongly spin dependent in presence of magnetic interaction. Occupation probabilities of all the Fe-d-orbitals exhibit temperature dependence indicating their possible contribution in orbital fluctuation. This need to be contrasted with the usual definition of nematic order parameter ($n_{d_{xz}} - n_{d_{yz}}$). Relationship among orbital fluctuations, magnetic fluctuations and nematicity are established.

© 2016 Elsevier B.V. All rights reserved.

1. Introduction

The discovery of high temperature superconductivity in Fe-based materials attaining T_c as large as 109K [1], has lead to a huge up surge of research for further discovery of such new materials [2]. Seven years after its discovery, while a clear consensus on the mechanism of superconductivity has not yet been reached, understanding on the structural, magnetic transitions and their mutual influences on superconductivity remain central issue of frontier research [2–4]. A large number of undoped Fe-based materials show spin density wave (SDW) magnetic state whose transition temperature coincides with that of the structural transition (which gets separated through doping as well as pressure). Both the transitions being second order in nature, can have a conflict with Landau theory of phase transition unless there would be a precursor transition at higher temperatures. According to Landau theory, occurrence of two simultaneous transitions may be purely coincidental, mutually independent, or one of the transitions be first order type or there must be a precursor to one of the

transitions at a higher temperature. What is that precursor?

Origin of the structural transition is not purely lattice driven but an electronic one; the orbital ordering of Fe d_{yz} and d_{xz} orbitals [5,6] is the primary reason for structural transition. Among some of the normal state properties, transport in "preferred" direction has been observed unambiguously in many experiments – inelastic neutron scattering (INS) [7], scanning tunnelling microscope, impurity [8], resistivity [9], optical conductivity [10], angle resolved photo electron spectroscopy [5] and so on. Overall, origin of such phenomena is related to the breaking of four-fold rotational (C_4) symmetry of the tetragonal phase known as nematicity – the precursor. Whether the origin of nematic phase is spin driven or orbital driven is far from being settled. The nematic phase is observed in FeSe materials, that has structural transition at 90 K but no trace of long-range magnetic order [11] indicating nematicity is orbital fluctuation driven [12]. However, observation of an additional C_4 phase deep inside the orthorhombic (C_2) phase in $\text{Ba}_{1-x}\text{Na}_x\text{Fe}_2\text{As}_2$ close to the suppression of magnetic spin density wave (SDW) order favours magnetically driven nematic order [13]. Role of nematic phase as regards to the mechanism of superconductivity or symmetry of Cooper pair wave function is not straight forward [14] but the fact that spin fluctuation leads to s^{+-} superconductivity

* Corresponding author.

E-mail address: hng@rrcat.gov.in (H. Ghosh).

[16] whereas the orbital fluctuation leads to s^{++} superconductivity in Fe-pnictides [17] are established and magnetism competes with superconductivity [18,19]. There are also evidences of 'nematic order' in the pseudogap phase of the other class of high temperature cuprates superconductors which are known to be strongly correlated materials [20–23]. On the other hand, 122 family of Fe-based superconductors are generally considered as weakly correlated systems. Therefore, the study of nematicity in Fe-based superconductors is of fundamental importance. Possible origins of nematic phase are well described in [3] as (a) structural distortion, (b) charge/orbital order, (c) spin order. Whatever be the nematic order parameter it must couple linearly to the orthorhombic distortion [24]. Nematicity introduces electronic anisotropy leading to two different nesting vectors which in turn leads to two competing spin density wave (SDW) instabilities ($Z_2 \times O(3)$ symmetry breaking) [25]. Coupling of the orbital order to SDW and vice versa has been used as inputs in Ginzburg-Landau formalism which provides qualitative understanding of nematic phase. A clear first principles understanding on whether there is any direct coupling between the magnetic (SDW) and orbital order in Fe-pnictides is absent till to date — is the main aim of this work.

We show through electronic structure calculation that the electronic orbital ordering locally breaks the in-plane symmetry and generate two non-equivalent a , b directions. In particular, we show that below structural transition (orthorhombic phase) there is a strong orbital anisotropy along the $\Gamma - X$ and $\Gamma - Y$ polarizations; the band at X is dominantly Fe- d_{yz} derived whereas that at Y , Fe- d_{xz} derived respectively. This feature reproduces correctly experimental angle resolved photo electron spectroscopy (ARPES) observation [5]. This is the root cause of orbital ordering in $\text{BaFe}_{2-x}\text{Ru}_x\text{As}_2$ — we show that the temperature dependence of the orbital ordering at $X(Y)$ point reproduces exactly that of orthorhombicity parameter (hence structural transition). Thus structural transition is primarily electronic in origin and phonons can not be a primary order parameter for nematicity. Whereas the temperature dependence of the same at Γ point is very weak (nearly independent of temperature) as observed experimentally [26]. Interestingly, Zhang et al. [26], observed that the orbital splitting (ordering) at Γ point (in case of FeSe) persists beyond structural transition temperature and argued that as against ferro-orbital ordering. In order to have a complementary first principles understanding over the experimental and other studies [3,5,7,12,13,26] we introduce magnetic interaction through tuning integrated spin density defined as, $I_s = \int (n_{\uparrow}(r) - n_{\downarrow}(r)) d^3r$. In presence of finite integrated spin density I_s , spin selective orbital ordering are observed. Due to electronic orbital anisotropy (see Fig. 3) the SDW state may be viewed as a superposition of two SDW states. This is because of two reasons, (i) nesting wave vector that connects nested parts of Fermi arcs along the $\Gamma - X$ and $\Gamma - Y$ directions are different; (ii) overlap of Fe- d_{xy} with d_{xz} and d_{yz} is different (below structural transition) causing anisotropic charge and spin density fluctuations. Tuning I_s causes further perturbation to the underlying SDW as well as splits the spin degeneracy of energy bands. This magnetic interaction couple with orbital (charge) fluctuations causing further orbital anisotropy. Remarkably, this later effect is observable only in the orthorhombic phase and not in the tetragonal phase. This would be experimentally verifiable by ARPES in presence of weak Zeeman field. In presence of I_s we evaluate thermal variations of orbital ordering at different high symmetry points. We show that the magnetic interaction couples to the zone centre orbital ordering very strongly where as it has a substantial effect on the corner zone orbital fluctuation. These observations support the claim by Zhang [26], Fernandes [3] of magnetic origin of nematic phase. Finally, we show that the orbital occupancies of all the five d-orbitals of Fe show temperature dependencies below structural transition. This

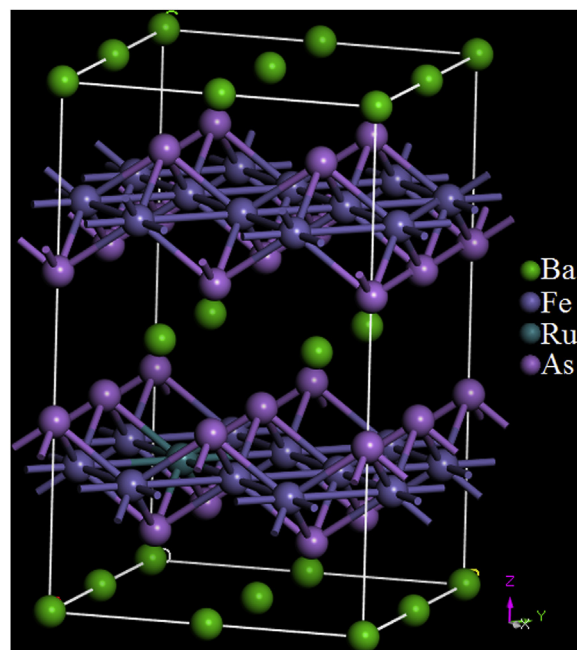


Fig. 1. Structure of a 40 atoms super-cell of BaFe_2As_2 , which contains 16 Fe atoms and one Ru atom corresponding to about 6% doping. Different colours are used to indicate different atoms.

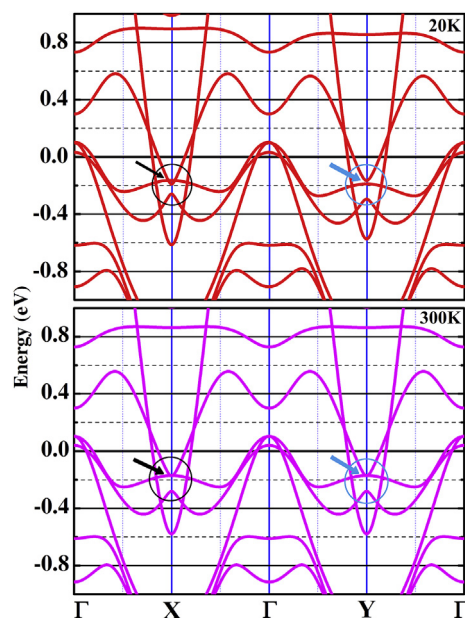


Fig. 2. Calculated band structure of BaFe_2As_2 along $\Gamma - X - \Gamma - Y - \Gamma$ direction at 20K (red) in orthorhombic phase and 300K (magenta) in tetragonal phase. Orbital anisotropy along $\Gamma - X$ and $\Gamma - Y$ direction in the orthorhombic phase is worth noticing. (For interpretation of the references to colour in this figure legend, the reader is referred to the web version of this article.)

indicates to the fact that nematic order parameter may not simply be defined as $(n_{d_{xz}} - n_{d_{yz}})$ but charge fluctuations from other orbitals also need to be considered, for example, the thermal variation of $(n_{d_{xz}} - n_{d_{yz}}) + (n_{d_{x^2-y^2}} - n_{d_{xy}})$ also follows orthorhombicity (see inset Fig. 5c). This will put constraints on many theoretical and experimental works so far.

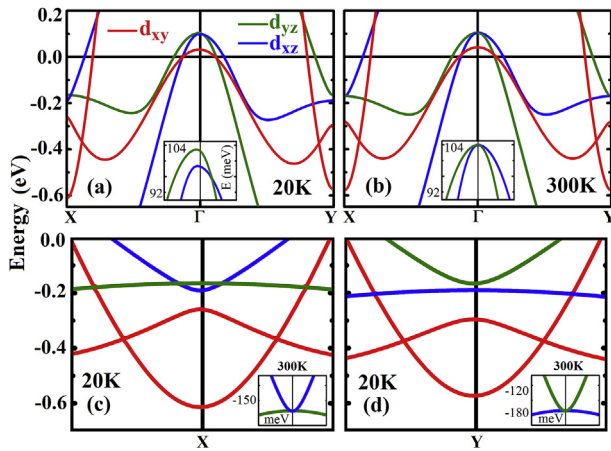


Fig. 3. Calculated band structure of BaFe_2As_2 along $\Gamma-X-\Gamma-Y-\Gamma$ direction at 20K (a) and 300K (b) indicating various d orbital (d_{yz} , d_{xz} and d_{xy}) using different colours. Orbital ordering in the orthorhombic phase is shown in the inset figure. Electronic orbital anisotropy at the X (c) and Y (d) points in the orthorhombic phase is the root cause of orbital order leading to structural transition.

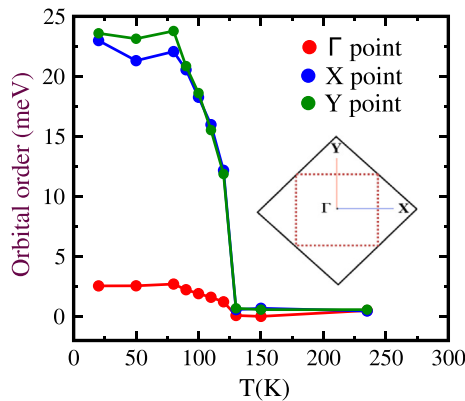


Fig. 4. Calculated orbital order (in meV) around X (blue), Y (green) and Γ (red) points as a function of temperature for 5% Ru doped BaFe_2As_2 . Brillouin zone of orthorhombic BaFe_2As_2 has been shown in the inset of the figure indicating various k points (X, Y and Γ). The temperature dependence of orbital order is same as that of orthorhombicity (δ) [30]. (For interpretation of the references to colour in this figure legend, the reader is referred to the web version of this article.)

2. Method

First principles density functional theories can produce exact solutions of the many electron Schrödinger equation if exact electronic density is being used as input. Various modern X-ray diffraction techniques e.g., Synchrotrons radiation source etc. that determines crystallographic information at different external perturbations are essentially result of diffraction from various atomic charge densities (Bragg's diffraction). Considering experimentally determined structural parameters at different temperatures as input thus in turn provides temperature dependent densities in our first principles calculation. These input structural parameters are kept fixed through out the calculation for a fixed temperature. This is how we use a $T = 0$ DFT formalism to bring out temperature dependent observable with the help of experimental input (energy being functional of electron density $E \equiv E[\rho(r, T)] \equiv E[\rho\{a(T), b(T), c(T)\}]$). The main effect on the electronic structure from finite temperature is the underlying crystal structure, and the average crystal structure at finite temperature can usually be reliably determined from the diffraction experiment at

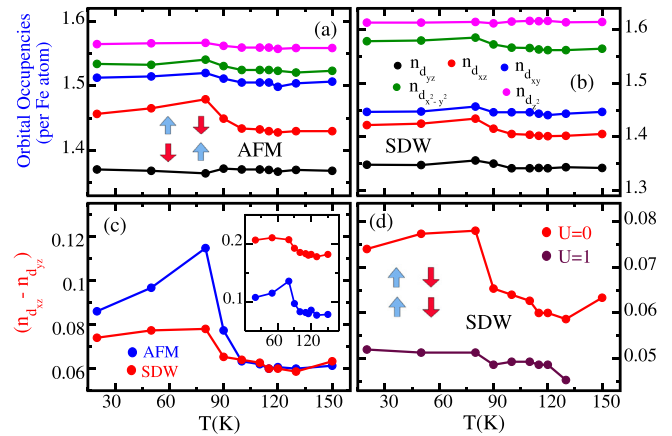


Fig. 5. Total orbital occupancies per Fe atom (in real space) of various d orbitals of all Fe-atoms in the super-cell as a function of temperature for (a) AFM and (b) SDW spin configuration indicated in the inset. (c) $(n_{d_{xz}} - n_{d_{yz}})$ and $(n_{d_{xz}} - n_{d_{yz}}) + (n_{d_{xz}} - n_{d_{yz}})$ (inset) as a function of temperature for AFM (blue) and SDW (red) spin structures. (d) Thermal variation of $(n_{d_{xz}} - n_{d_{yz}})$ for SDW spin configuration considering correlation ($U = 1$) using GGA + U formalism and with out correlation. (For interpretation of the references to colour in this figure legend, the reader is referred to the web version of this article.)

a given temperature. This method is somewhat superior to other similar methodology, like molecular dynamics simulation (MD). Through MD simulation one finds temperature dependent lattice parameters and then use standard $T = 0$ DFT method using GGA exchange potential (see for example [27–30,6]). However, experimentally determined temperature dependent lattice parameters can be obtained with an accuracy better than 0.001 Å which may not be possible in MD. Using temperature and doping dependent experimental lattice parameters $a(T, x)$, $b(T, x)$, $c(T, x)$ and $z_{\text{As}}(T, x)$ [30], we obtain electronic structure as a function of temperature as well as doping, to explain the experimentally observed anomalies microscopically. One of the shortcomings of the density functional theory (DFT) under generalized gradient approximation (GGA) for calculating electronic structures of Fe-based SCs is that it fails to reproduce accurate experimental z_{As} [31,32,30,33]. This conflict arises due to strong magnetic fluctuation associated with Fe based compounds [34]. This insist us to take experimental z_{As} instead of relaxed z_{As} obtained by total energy minimization, as one of our input parameters. We simulate electronic structures for both the phases, low temperature orthorhombic phase with anti-ferromagnetic (AFM) as well as spin density wave (SDW) ordering and high temperature paramagnetic tetragonal phase. In low temperature orthorhombic phase, along with non magnetic structures various spin configurations have been employed among which the lowest energy configuration is considered for electronic structure calculation. Our first principles electronic structure calculations are carried out implementing plane-wave pseudopotential method within the framework of density functional theory [35]. In all of our temperature and doping dependent calculations the electronic exchange correlation energy is treated under the generalized gradient approximation (GGA) using Perdew-Burke-Ernzerhof (PBE) functional [36]. Tackling small fraction of Ru substitution in place of Fe is accomplished by considering both, the virtual crystal approximation (VCA) as well as super-cell method for convenience. Super-cell method is a computationally expensive method adopted to mimic finite percentage of doping at a particular site. Lets say e. g, for 5% doping at the Fe site one needs to build a super-cell (bigger unit cell) that contains 20 Fe atoms; then 1 of the Fe atoms are replaced by Ru atom (say). In the

present case however, a super-cell containing 16 Fe atoms (total 40 atoms) are taken out of which one is replaced by a Ru (shown in Fig. 1). This corresponds to 6% Ru doping which is close to the experimental situation. Note the size of the unit cell in the given symmetry is such that it does not allow exactly a super-cell with 20 Fe atoms.

Spin polarized single point energy calculations are performed using AFM and SDW configuration [37] (see inset Fig. 5) for the low temperature orthorhombic phase with space group symmetry Fmmm (No.69) using ultrasoft pseudopotentials. Plane wave basis set with energy cut off 500 eV and self consistent field (SCF) tolerance 10^{-6} eV/atom has been opted for all calculations. Brillouin zone is sampled in the k space within Monkhorst-Pack scheme and grid size for SCF calculation is $12 \times 12 \times 12$ for electronic density of state calculation in primitive cell for orthorhombic phase. Band structure calculations are performed along various k -paths (X , Γ and Y) with k point separation 10^{-6} Å. Standard rotationally invariant approach due to Matteo Cococcioni and Stefano de Gironcoli [38] and V. I. Anisimov [39] is used to treat the Hubbard on site repulsion effect by post-DFT LSDA + U method which calculates and uses the total spin-projected occupation of the localized manifold, as this is essential to treat the Hubbard term. Therefore, the method of calculation of occupation probabilities of U effected orbitals remain same as that of the reference given above which is also valid even in the limit U tending to zero.

3. Results and discussions

First, we have calculated band structures of BaFe_2As_2 system for anti-ferromagnetic (AFM) spin configuration (total spin zero) using experimental lattice parameters at 20K as well as 300K along some specified k -path to probe orbital anisotropy. Our calculated band structures of BaFe_2As_2 along the k path $\Gamma - X - \Gamma - Y - \Gamma$ at two different temperatures corresponding to orthorhombic and tetragonal (20K and 300K) phases respectively are shown in Fig. 2. Circular envelopes are drawn around high symmetry X, Y points which are then shown in Fig. 3 where splitting of d_{xz}/d_{yz} at Γ point has also been highlighted. It is very clear from Fig. 3a that at 20K (orthorhombic phase), band dispersion along $\Gamma - X$ direction is quite different compared to that in the $\Gamma - Y$ direction. In Fig. 3 the splitting of d_{xz}/d_{yz} at Γ point has also been highlighted in the inset. The same for the room temperature is then compared with. Fig. 3 demonstrate that the orbital ordering locally breaks the in plane symmetry and generates two non-equivalent a, b directions \perp to c . This results in two different nesting wave vectors along $Q_x = (\pi, 0)$ and $Q_y = (0, \pi)$ directions - that is spins are parallel to each other along X -direction and anti-parallel along Y -direction (O_3). We would also like to mention that at lower temperatures there exists two Fe-Fe distances (Z_2) [6,30] and this makes the system anisotropic both magnetically as well as in terms of band motion. This situation resembles to that of the nematic phase where the bilinear combination of the order parameter ($O_3 \times Z_2$) breaks the tetragonal symmetry and is invariant under symmetry transformation. Because of the anisotropy of the bands along X and Y directions, in general, (overlap of the d_{xy} band with d_{xz} and d_{yz} bands are specially different) causes inter-band charge and spin fluctuations, which may cause for example, coupling between them resulting in different amplitudes of the SDW along Q_x and Q_y directions. Energy orderings of the non-degenerate d_{xz}/d_{yz} bands sets in orbital ordering [6,40,15], temperature dependence of which defines structural transition. This is depicted in Fig. 4. It should be clearly noted that the structural distortion is predominantly determined by the orbital ordering at $X(Y)$ point; it is very weakly influenced by the orbital ordering at Γ point which has very weak temperature dependence. This clearly shows that the orbital ordering is very

anisotropic. Now, question is why is that the orbital ordering at the (zone centre) Γ point is so weak but finite and independent of temperature? This is also observed experimentally by Zhang et al. [26], and modelled as bond-order. We argue below this as manifestations of orbital anisotropy in presence of zone folding due to magnetic order. It is easy to envisage from the band structure in Fig. 3 that because of interband nesting $E_{d_{xz}}(k + Q_x) = -E_{d_{xz}}(k)$, but $E_{d_{yz}}(k + Q_x) = -E_{d_{xz}}(k)$ and $E_{d_{xz}}(k + Q_y) = -E_{d_{yz}}(k)$, but $E_{d_{yz}}(k + Q_y) = -E_{d_{yz}}(k)$. These would make the nematic order parameter ($n_{d_{xz}} - n_{d_{yz}}$) null if the nesting wave vectors Q_x, Q_y were equivalent, but as it is not, it results in some small but finite quantity which is nearly independent of temperature. This feature is indicative of the fact that the orbital ordering 'gap' would form a density wave and this along with the SDW state is interband in nature [18].

By now through above discussions it is nearly evident as to what is the source of temperature dependence of the orbital order parameter and may relate to the same of the nematic order parameter. The Fe band energies presented in Fig. 3 may be written as, $E(k) = \sum_i \epsilon_i(k) n_i(k)$; $i = d_{xz}, d_{yz}, d_{xy}, d_{x^2-y^2}, d_{(3z^2-r^2)}$ and the corresponding eigenstates involving orbitals are $\Psi = \sum_i c_i \phi_i \cdot \epsilon_i(k)$ and $n_i(k)$ s are the band energies and occupation probabilities of i 'th orbital ϕ_i respectively. The $\epsilon_i(r)$ s being the Kohn-Sham orbit energies and the corresponding Fourier transformed $\epsilon_i(k)$ s are independent of temperature (and magnetic interaction introduced later through I_s), whereas the orbital occupancies (or densities) $n_i(k)$ are function of temperature. Therefore, lifting of degeneracy of the d_{xz}, d_{yz} bands at the Γ and X points, as the temperature is lowered below structural transition temperature is a consequence of the fact that their occupation probabilities become different (i.e. partial densities become unequal). Note, the energy gap between the d_{xz}, d_{yz} bands at the Γ and X points is a function of temperature (see Fig. 4). The temperature difference essentially originates from the temperature dependencies of $n_{d_{xz}}, n_{d_{yz}}$ and is proportional to $n_{d_{xz}} - n_{d_{yz}}$ (see Fig. 5c). Therefore, it is desirable to calculate the temperature dependencies of the occupation probabilities of all the five d -orbitals of Fe from first principles calculation. Such a rare calculation is presented in Fig. 5. This quantity ($n_{d_{xz}} - n_{d_{yz}}$) represents inter orbital charge fluctuation or orbital fluctuation in short, one of the important contender for nematic phase and is also called nematic order parameter. Using super-cell of orthorhombic BaFe_2As_2 structure corresponding to $\sim 6\%$ Ru doping (cf. Fig. 1) and two types of spin arrangements AFM and SDW (shown in the inset of Fig. 5) first principles simulations of orbital occupancies are presented.

Why dope BaFe_2As_2 with Ru? Like hole doped 122 systems iso-electronic Ru doped 122 system also have inseparably same structural and magnetic transitions and the nematic phase in this system remain unexplored. This is unlike other iso-electronic P doping in place of As. It is particularly an interesting case, it is not clear as to where does the charge carrier go in case of Ru doping in place of Fe. Both the hole and electron Fermi pockets either remain unaltered or expands at an equal rate [28,33]. Furthermore, both the structural and magnetic transitions are 2nd order in nature in case of underdoped Ru-122 system. Therefore, study of temperature dependence of orbital fluctuation from first principles is of genuine interest. In Fig. 5 orbital occupancies of d_{xz} orbital ($n_{d_{xz}}$) modifies significantly with temperature compared to the other d orbitals specially d_{yz} and d_{xy} (but they also do show substantial temperature dependence). We have also calculated the difference in the occupancies of d_{xz} and d_{yz} orbitals i. e. $n_{d_{xz}} - n_{d_{yz}}$ (nematicity) as a function of temperature for both AFM and SDW spin configuration (see Fig. 5c). Since, above structural transition there is no splitting between the d_{xz} and d_{yz} bands (i.e. $\epsilon_{xz} = \epsilon_{yz}$) temperature dependence of the nematic order parameter $n_{d_{xz}} - n_{d_{yz}}$ is

proportional to that of the orbital order. In other words, the nematic order essentially grow as orbital order which is responsible for orthorhombic transition. Therefore, this result may be interpreted as the first principles evidence of the fact that if orbital fluctuation is the primary order responsible for nematicity, then it is proportional to the orthorhombicity parameter [3]. This is one of the inputs of all the theories involving Ginzburg Landau formalism. As already mentioned towards the end of theoretical method section that the method of calculation of occupation probabilities of U effected orbitals remains same as that of the ref. [38,39] which is also valid even in the limit U tending to zero. Therefore, occupation probabilities are obtained for a very small $U = 0.01\text{eV}$ (not exactly equal to zero) which makes up/down spin states different even in the tetragonal phase. As a result $n_{d_{xz}} - n_{d_{yz}}$ become very small but non-zero and has hardly any temperature dependence. Also, the difference in the nematic order parameter for SDW and AFM clearly indicates that it is a spin nematicity. Furthermore, in the inset of Fig. 5c, we depict the thermal variation of $(n_{d_{xz}} - n_{d_{yz}}) + (n_{d_{x^2-y^2}} - n_{d_{xy}})$ which also reproduces thermal behaviour of orthorhombicity corresponding to orbital fluctuation involving all four d-orbitals. Thus, in contrast to the usual belief in literature, nematic order parameter which is defined as $n_{d_{xz}} - n_{d_{yz}}$, perhaps involve all other d-orbitals as well.

The nematic order parameters show substantial modifications near the temperature where magnetic fluctuation is very strong (see Fig. 8). This provides a distinct evidence to the fact that probably magnetic fluctuation, orbital fluctuation, the nematicity are interdependent (we discuss this issue below). Also it should be noted that the orbital occupancies of d_{xz} orbital is always greater than that of the d_{yz} orbital i.e., $n_{d_{xz}} > n_{d_{yz}}$. This propound ferro-orbital ordering. Partial densities n_{xz} , n_{yz} being unequal would correspond to different bonding along x and y directions, a mark of nematicity due to orbital anisotropy. Unlike cuprates it is experimentally well established that 122 family of Fe-based SCs are weakly correlated. In Fig. 5d temperature dependence of $n_{d_{xz}} - n_{d_{yz}}$ has been shown with small on site correlation ($U = 1$) and with out correlation. It is clear that correlation reduces orbital order and so the magnetic fluctuation (see Fig. 6b). Magnetic fluctuations play an important role in these family of Fe-based SCs. Stoner factor is the measure of these magnetic fluctuation. Stoner factor of this compound can be defined as $I^{\text{Fe}} \times [N^{\text{Fe}}(E_F)]^2 + I^{\text{Ru}} \times [N^{\text{Ru}}(E_F)]^2$, where $N^{\text{Fe}}(E_F)$ and $N^{\text{Ru}}(E_F)$ are the density of states at the Fermi level from Fe and Ru atoms respectively [41,42]. The value of Stoner parameters I^{Fe} and I^{Ru} are taken from ref [41,43]. We have calculated the Stoner factor as a function of temperature and displayed in Fig. 6a. As temperature changes, partial density of states of Fe and Ru at the Fermi level (E_F) get modified due to substantial moderation of Fe-As hybridization. This is the root cause of temperature dependence of Stoner factor. This observation is very much consistent with recent experimental findings [44]. In Fig. 6b thermal variation of Stoner

factor has been depicted with different values of U (strength of electron correlation). It is clear that with increasing electron repulsion (system would prefer stable antiferromagnetic configuration) magnetic fluctuation is actually decreasing (so is the nematic order) which enhances further our suspect that magnetic fluctuation triggers orbital fluctuation and nematic phase. For this purpose, we tune magnetic interaction manually by introducing integrated spin density parameter as explained above and see its influence on electronic structure. While keeping initial AFM spin structure we provide constraint through the integrated spin density parameter for spin polarized calculations which induces some magnetic moment in the system. This method is a simple extension of standard LSDA formalism where total energy as a function of moment can be obtained. After complete spin polarized calculation being performed, the main idea is to perform a single point energy calculation keeping the total moment constrained to some fixed small but finite non zero values. This is equivalent to generating a weak Zeeman field (see also the form of the integrated spin density parameter). In this way by keeping the AFM spin configuration, magnetic interaction can be introduced to the system by simply fixing the total (difference in up and down spin) magnetic moment of the system through integrated spin density parameter. Actually, from electronic structure calculation we calculate orbital ordering again in presence of magnetic interaction (see below) and see that orbital anisotropy is enhanced, and hence the nematicity.

In presence of finite integrated spin density, the band of up spin electrons and band of down spin electrons split. We observed that for $I_s = 1$ and 2, one of the bands (up spin) goes deep below the Fermi level. So only one of the spin electronic bands are contributing significantly at the Fermi level. In Fig. 7 we have shown the band structures of 5% Ru doped BaFe_2As_2 systems at 20 K, $I_s = 1$ for down spin (left) and up spin (right) electrons around different k points (X, Y and Γ points). Notably, around X, Y and Γ points all the orbitals are ordered differently in contrast to that in Fig. 3. Around X as well as around Γ point the energy ordering of d_{xz} and d_{yz} orbitals are exactly opposite to each other for up spin and down spin bands. This leads to spin-polarized orbital orderings (possibly orbital density wave). We do all the same exercises (in all the figures above) for K doped as well as P doped 122 systems and found that the orbital ordering is a common phenomena (there are differences in details and will be reported elsewhere). In Fig. 8 we have presented temperature variation of orbital order around X, Y and Γ points for $I_s = 1$ (Fig. 8a) and $I_s = 2$ respectively (Fig. 8b) after extracting the required information from Fig. 7. In case of $I_s = 1$ the orbital order around Γ increases to about 3 fold compared to the case where we optimized the total spin of the system (represented by hollow symbols). However, the orbital ordering around the zone corners X(Y) are less affected. When the integrated spin density is increased to 1 from 0, it stabilizes the underlying SDW, but when I_s is further increased to 2, the underlying SDW ordering will be strongly suppressed due to ferromagnetic nature of the I_s . Hence, orbital ordering is strongly coupled to the underlying magnetic fluctuation (it enhances orbital fluctuation or nematic order parameter) and our study thus is complementary to recent studies [3,5,26,45,46] on nematic phase.

4. Conclusion

We establish the microscopic relationship between the orbital order, structural transition and nematic order in 122 family of Fe-based superconductors. While electronic orbital anisotropy gives rise to orbital order, temperature dependence of the orbital order is found to be exactly same as that of the orthorhombicity, indicating orbital ordering is responsible for structural transition. Temperature dependence of the orbital order is proportional to the

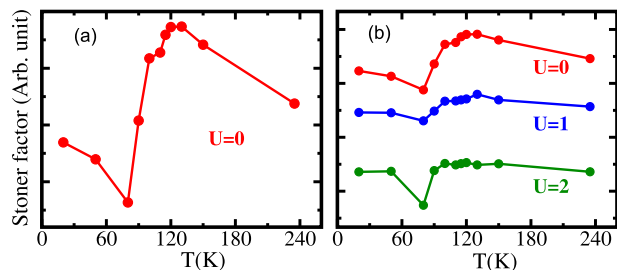


Fig. 6. (a) Calculated Stoner factor ($I^{\text{Fe}} \times [N^{\text{Fe}}(E_F)]^2 + I^{\text{Ru}} \times [N^{\text{Ru}}(E_F)]^2$) as a function of temperature for 5% Ru doped BaFe_2As_2 systems and (b) thermal variation of Stoner factor for different U values as indicated in the figure.

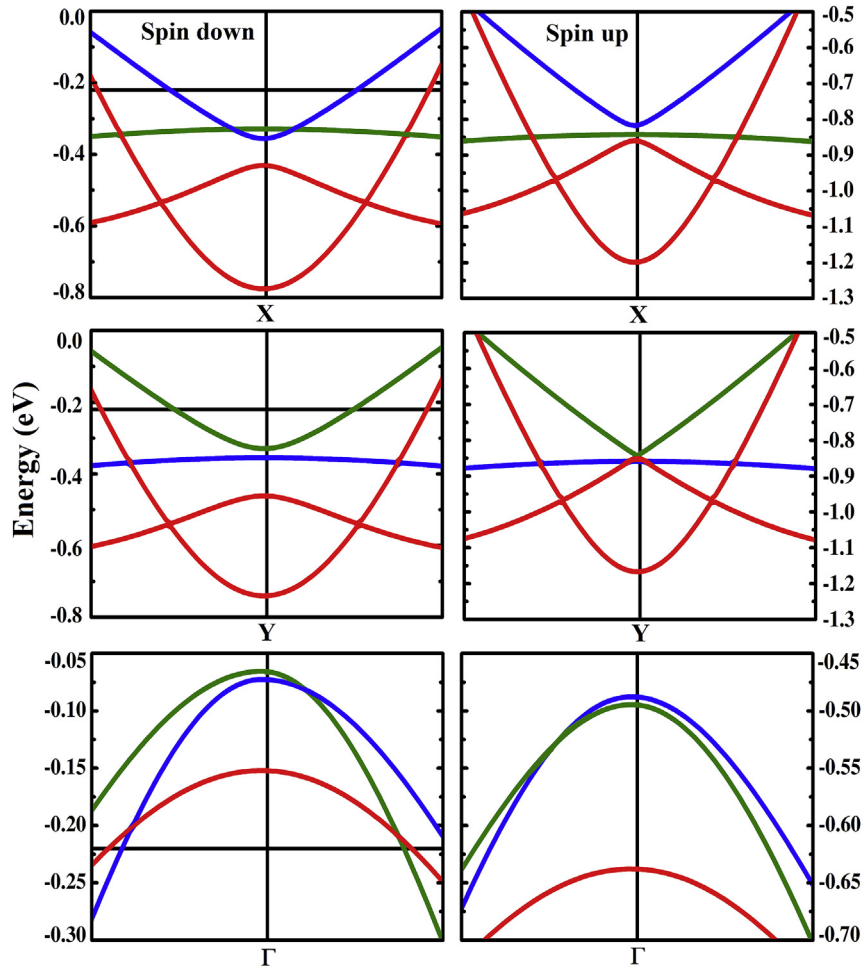


Fig. 7. Calculated band structure of 5% Ru doped BaFe₂As₂ systems at 20 K with $I_s = 1$ for down spin (left) and up spin (right) electrons around X, Y and Γ points. We assign red green and blue colours to d_{xy} , d_{yz} and d_{xz} orbitals respectively. (For interpretation of the references to colour in this figure legend, the reader is referred to the web version of this article.)

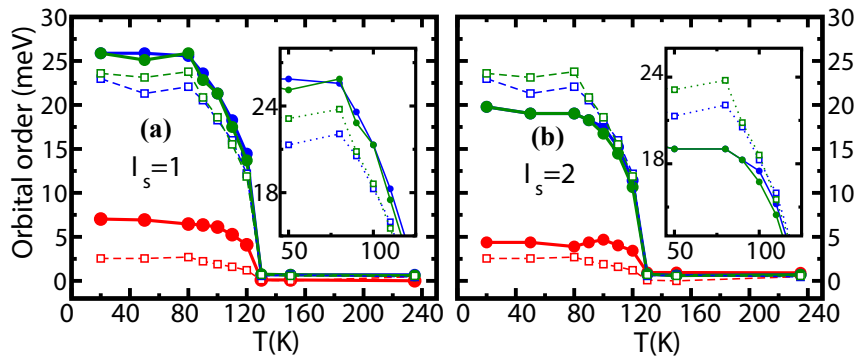


Fig. 8. Calculated orbital order (in meV) around X (blue), Y (green) and Γ (red) points as a function of temperature for (a) $I_s = 1$ and (b) $I_s = 2$ for 5% Ru doped BaFe₂As₂ systems. Hollow symbols represent data from Fig. 4. (For interpretation of the references to colour in this figure legend, the reader is referred to the web version of this article.)

temperature dependence of the nematic order ($n_{d_{xz}} - n_{d_{yz}}$). This indicates that the nematic order grows as orbital order in the orthorhombic phase. We have explicitly evaluated the temperature dependencies of orbital occupancies of all Fe-d-orbitals. Almost all the d-orbitals show substantial charge fluctuations in the orthorhombic phase, indicating that the actual definition of nematic order parameter may be more complicated. The nematic order parameter is found to show temperature dependence close to the

onset of magnetic fluctuation, obtained rigorously through evaluation of Stoner factor. When magnetic fluctuations are enhanced, the orbital fluctuations are also enhanced and vice versa establishing their couplings. Spin-polarised orbital ordering revealed from this work would be experimentally observable. Finally, our work supports magnetic origin of nematicity in 122 family of Fe-based superconductors. We believe this work would generate further interest in theoretical as well as experimental studies.

Competing financial interests

The authors declare no competing financial interests.

Acknowledgements

We thank Dr. A. Bharathi and Dr. A. K. Sinha for discussion on experimental aspects. We thank Dr. P. A. Naik and Dr. P. D. Gupta for their encouragement in this work. One of us (SS) acknowledges the HBNI, RRCAT for financial support and encouragements.

References

- [1] Jian-Feng Ge, Zhi-Long Liu, Canhua Liu, Chun-Lei Gao, Dong Qian, Qi-Kun Xue, Ying Liu, Jin-Feng Jia, Superconductivity above 100K in single-layer FeSe films on doped SrTiO₃, *Nat. Mater.* 14 (2015) 285–289.
- [2] Hideo Hosono, Keiichi Tanabe, Eiji Takayama-Muromachi, Hiroshi Kageyama, Shoji Yamanaka, Hiroshi Kumakura, Minoru Nahara, Hidenori Hiramatsu, Satoru Fujitsu, Exploration of new superconductors and functional materials, and fabrication of superconducting tapes and wires of iron pnictides, *Sci. Technol. Adv. Mater.* 16 (2015) 033503–033589.
- [3] R.M. Fernandes, A.V. Chubukov, J. Schmalian, What drives nematic order in iron-based superconductors, *Nat. Phys.* 10 (2014) 97–104.
- [4] J.J. Wu, Jung-Fu Lin, X.C. Wang, Q.Q. Liu, J.L. Zhu, Y.M. Xiao, P. Chow, Changqing Jin, Pressure-decoupled magnetic and structural transitions of the parent compound of iron-based 122 superconductors BaFe₂As₂, *Proc. Natl. Acad. Sci. U. S. A.* 110 (43) (2013) 17263–17266.
- [5] Ming Yia, Donghui Lu, Jiun-Haw Chua, James G. Analytis, Adam P. Sorini, Alexander F. Kemper, Brian Moritz, Sung-Kwan Mo, Rob G. Moore, Makoto Hashimoto, Wei-Sheng Lee, Zahid Hussain, Thomas P. Devereaux, Ian R. Fisher, Zhi-Xun Shen, Symmetry-breaking orbital anisotropy observed for detwinned Ba(Fe_{1-x}Co_x)₂As₂ above the spin density wave transition, *Proc. Natl. Acad. Sci. U. S. A.* 108 (17) (2011) 6878–6883.
- [6] Smritijit Sen, Haranath Ghosh, A.K. Sinha, A. Bharathi, Origin of structural and magnetic transitions in BaFe_{2-x}Ru_xAs₂ materials, *Supercond. Sci. Technol. (Fast Track Commun.)* 27 (2014), 122003–12009.
- [7] Jun Zhao, Dao-Xin Yao, Shiliang Li, Tao Hong, Y. Chen, S. Chang, W. Ratcliff II, J.W. Lynn, H.A. Mook, G.F. Chen, J.L. Luo, N.L. Wang, E.W. Carlson, Jiangping Hu, Pengcheng Dai, Low energy spin waves and magnetic interactions in SrFe₂As₂, *Phys. Rev. Lett.* 101 (2008) 167203–167206.
- [8] M.P. Allan, T.-M. Chuang, F. Massee, Yang Xie, Ni Ni, S.L. Budko, G.S. Boebinger, Q. Wang, D.S. Dessau, P.C. Canfield, M.S. Golden, J.C. Davis, Anisotropic impurity states, quasiparticle scattering and nematic transport in underdoped Ca(Fe_{1-x}Co_x)₂As₂, *Nat. Phys.* 9 (2013) 220–224.
- [9] Jiun-Haw Chu, James G. Analytis, Kristiaan De Greve, Peter L. McMahon, Zahirul Islam, Yoshihisa Yamamoto, Ian R. Fisher, In-plane resistivity anisotropy in an underdoped iron arsenide superconductor, *Sci.* 329 (2010) 824–826.
- [10] A. Dusza, A. Lucarelli, A. Sanna, S. Massidda, J.-H. Chu, I. R. Fisher, L. Degiorgi, Anisotropic in-plane optical conductivity in detwinned Ba(Fe_{1-x}Co_x)₂As₂, *New J. Phys.* 14 (2012) 023020–023039.
- [11] Can-Li Song, Yi-Lin Wang, Peng Cheng, Ye-Ping Jiang, Wei Li, Tong Zhang, Zhi Li, Ke He, Lili Wang, Jin-Feng Jia, Hsiang-Hsuan Hung, Congjun Wu, Xucun Ma, Xi Chen, Qi-Kun Xue, Direct observation of nodes and twofold symmetry in FeSe superconductor, *Sci.* 332 (2011) 1410–1413.
- [12] S.-H. Baek, D.V. Efremov, J.M. Ok, J.S. Kim, Jeroen van den Brink, B. Büchner, Orbital-driven nematicity in FeSe, *Nat. Mater.* 14 (2015) 210–214.
- [13] S. Avci, O. Chmaissem, J.M. Allred, S. Rosenkranz, I. Eremin, A.V. Chubukov, D.E. Bugaris, D.Y. Chung, M.G. Kanatzidis, J.-P. Castellan, J.A. Schlueter, H. Claus, D.D. Khalyavin, P. Manuel, A. Daoud-Aladine, R. Osborn, Magnetically driven suppression of nematic order in an iron-based superconductor, *Nat. Commun.* 5 (2014) 3845–3850.
- [14] T. Shimojima, F. Sakaguchi, K. Ishizaka, Y. Ishida, T. Kiss, M. Okawa, T. Togashi, C.-T. Chen, S. Watanabe, M. Arita, K. Shimada, H. Namatame, M. Taniguchi, K. Ohgushi, S. Kasahara, T. Terashima, T. Shibauchi, Y. Matsuda, A. Chainani, S. Shin, Orbital-independent superconducting gaps in iron pnictides, *Sci.* 332 (2011) 564–567.
- [15] Y. Suzuki, T. Shimojima, T. Sonobe, A. Nakamura, M. Sakano, H. Tsuji, J. Omachi, K. Yoshioka, M. Kuwata-Gonokami, T. Watashige, R. Kobayashi, S. Kasahara, T. Shibauchi, Y. Matsuda, Y. Yamakawa, H. Kontani, K. Ishizak, Momentum-dependent sign inversion of orbital order in superconducting FeSe, *Phys. Rev. B* 92 (2015) 205117.
- [16] I.I. Mazin, D.J. Singh, M.D. Johannes, M.H. Du, Unconventional Superconductivity with a Sign Reversal in the Order Parameter of LaFeAsO_{1-x}F_x, *Phys. Rev. Lett.* 101 (2008) 057003–057006.
- [17] H. Kontani, S. Onari, Orbital-fluctuation-mediated superconductivity in iron pnictides: analysis of the five-orbital Hubbard–Holstein model, *Phys. Rev. Lett.* 104 (2010) 157001–157004.
- [18] Haranath Ghosh, H. Purwar, Elementary and collective excitations as probes for order parameter symmetry in Fe-based superconductors, *Europhys. Lett.* 98 (2012) 57012–57017.
- [19] R.M. Fernandes, J. Schmalian, Competing order and nature of the pairing state in the iron pnictides, *Phys. Rev. B* 82 (2010) 014521–014542.
- [20] M.J. Lawler, et al., Intra-unit-cell electron nematicity of the high-T_c copper-oxide pseudogap states, *Nat.* 466 (2010) 347–351.
- [21] V. Hinkov, et al., Electronic liquid crystal state in the high-temperature superconductor YBa₂Cu₃O_{6.45}, *Sci.* 319 (2008) 597–600.
- [22] R. Daou, et al., Broken rotational symmetry in the pseudogap phase of a high-T_c superconductor, *Nat.* 463 (2010) 519–522.
- [23] K. Fujita, et al., Simultaneous transitions in the cuprate momentum-space topology and electronic symmetry breaking, *Sci.* 344 (2014) 612–616.
- [24] R.M. Fernandes, et al., Effects of nematic fluctuations on the elastic properties of iron arsenide superconductors, *Phys. Rev. Lett.* 105 (2010) 157003–157006.
- [25] R.M. Fernandes, S. Maiti, P. Wölfle, A.V. Chubukov, How many quantum phase transitions exist inside the superconducting dome of the iron pnictides? *Phys. Rev. Lett.* 111 (2013) 057001–057005.
- [26] P. Zhang, et al., Observation of two distinct d_{xz}/d_{yz} band splittings in FeSe, *Phys. Rev. B* 91 (2015) 214503–214507.
- [27] S. Backes, Harald O. Jeschke, Finite temperature and pressure molecular dynamics for Ba₂As₂, *Phys. Rev. B* 88 (2013) 075111–075118.
- [28] R.S. Dhaka, S.E. Hahn, E. Razzoli, Rui Jiang, M. Shi, B.N. Harmon, A. Thaler, S.L. Budko, P.C. Canfield, Adam Kaminski, Unusual temperature dependence of band dispersion in Ba(Fe_{1-x}Ru_x)₂As₂ and its consequences for antiferromagnetic ordering, *Phys. Rev. Lett.* 110 (2013) 067002–067006.
- [29] Jonathan M. Skelton, Stephen C. Parker, Atsushi Togo, Isao Tanaka, Aron Walsh, Thermal physics of the lead chalcogenides PbS, PbSe, and PbTe from first principles, *Phys. Rev. B* 89 (2014) 205203.
- [30] S. Sharma, A. Bharathi, K. Vinod, C.S. Sundar, V. Srihari, S. Sen, H. Ghosh, A.K. Sinha, S.K. Deb, Structural investigations in BaFe_{2-x}Ru_xAs₂ as a function of Ru and temperature, *Acta Cryst. B* 71 (2015) 61–67.
- [31] L. Zhang, D.J. Singh, Electronic structure of Ba(Fe,Ru)₂As₂ and Sr(Fe,Ir)₂As₂ alloys, *Phys. Rev. B* 79 (2009) 174530–174534.
- [32] Z.P. Yin, et al., Electron-hole symmetry and magnetic coupling in antiferromagnetic LaFeAsO, *Phys. Rev. Lett.* 101 (2008) 047001–047004.
- [33] Smritijit Sen, Haranath Ghosh, Fermiology of 122 family of Fe-based superconductors: an *ab initio* study, *Phys. Lett. A* 379 (2012) 843–847.
- [34] I.I. Mazin, M.D. Johannes, L. Boeri, K. Koepernik, D.J. Singh, Problems with reconciling density functional theory calculations with experiment in ferropnictides, *Phys. Rev. B* 78 (2008) 085104–085110.
- [35] S.J. Clark, et al., First principles methods using CASTEP, *Z. fuer Kristallogr.* 220 (2005) 567–570.
- [36] J.P. Perdew, K. Burke, M. Ernzerhof, Generalized gradient approximation made simple, *Phys. Rev. Lett.* 77 (1996) 3865–3868.
- [37] P. Dai, J. Hu, E. Dagotto, Magnetism and its microscopic origin in iron-based high-temperature superconductors, *Nat. Phys.* 8 (2012) 709–718.
- [38] Matteo Cococcioni, Stefano de Gironcoli, Linear response approach to the calculation of the effective interaction parameters in the LDA+U method, *Phys. Rev. B* 71 (2005) 035105–035120.
- [39] Vladimir I. Anisimov, Jan Zaanen, Ole K. Andersen, Band theory and Mott insulators: Hubbard U instead of Stoner I, *Phys. Rev. B* 44 (1991) 943–954.
- [40] T. Shimojima, K. Ishizaka, Y. Ishida, N. Katayama, K. Ohgushi, T. Kiss, M. Okawa, T. Togashi, X.-Y. Wang, C.-T. Chen, S. Watanabe, R. Kadota, T. Oguchi, A. Chainani, S. Shin, Orbital-dependent modifications of electronic structure across the magnetostructural transition in BaFe₂As₂, *Phys. Rev. Lett.* 104 (2010) 057002–057005.
- [41] O.K. Andersen, J. Madsen, U.K. Poulsen, O. Jepsen, J. Kollár, *Phys. C* 86–88 (1977) 249–256; [41a] E. C.Stoner, Collective electron ferromagnetism, *Proc. R. Soc. A Math. Phys. Eng. Sci.* 165(1938), 372–414.
- [42] Guangtao Wang, Lihua Zheng, Mingping Zhang, Zongxian Yang, Suppression of magnetism in SrFe_{2-x}Ru_xAs₂: first-principles calculations, *Phys. Rev. B* 81 (2010) 014521–014525.
- [43] J.-Q. Yan, A. Kreyssig, S. Nandi, N. Ni, S.L. Budko, A. Kracher, R.J. McQueeney, R.W. McCallum, T.A. Lograsso, A.I. Goldman, P.C. Canfield, Structural transition and anisotropic properties of single-crystalline SrFe₂As₂, *Phys. Rev. B* 78 (2008) 024516–024519.
- [44] K. Matan, R. Morinaga, K. Iida, T.J. Sato, Anisotropic itinerant magnetism and spin fluctuations in BaFe₂As₂: a neutron scattering study, *Phys. Rev. B* 79 (2009) 054526–054532.
- [45] Huiqian Luo, Meng Wang, Chenglin Zhang, Xingye Lu, Louis-Pierre Regnault, Rui Zhang, Shiliang Li, Jiangping Hu, Pengcheng Dai, Spin excitation anisotropy as a probe of orbital ordering in the paramagnetic tetragonal phase of superconducting BaFe_{1.904}Ni_{0.096}As₂, *Phys. Rev. Lett.* 111 (2013) 107006–107011.
- [46] Xingye Lu, J.T. Park, Rui Zhang, Huiqian Luo, Andriy H. Nevidomskyy, Qimiao Si, Pengcheng Dai, Nematic spin correlations in the tetragonal state of uniaxial-strained BaFe_{2-x}Ni_xAs₂, *Sci.* 345 (2014) 657–660.